Supporting information: Evaluation of ZIF-8 flexible force fields for structural and mechanical properties

E. Acuna Yeomans,[†] J. J. Gutierrez-Sevillano,[‡] S. Calero,[*,†,‡] and D. Dubbeldam[¶]

†*Department of Applied Physics, Eindhoven University of Technology, Eindhoven, Netherlands*

‡*Department of Physical, Chemical, and Natural Systems, University Pablo de Olavide, Seville, Spain*

¶*Van 't Hoff Institute for Molecular Sciences, University of Amsterdam, Amsterdam, Netherlands*

E-mail: S.Calero@tue.nl

Description of the force fields

This section contains the description of functional forms and corresponding parameter sets of the five ZIF-8 force fields used in this study, taken from the literature, as well as notes regarding their implementation in both RASPA and LAMMPS.

As is the case in the main manuscript, for organizational and convenience purposes the following nomenclature will be used:

- **FF1** : B. Zheng *et al.* (2012)[1]
- **FF2** : J. Jiang *et al.* (2012)[2]
- **FF3** : L. Zhang *et al.* (2013)[3]
- **FF4** : X. Wu *et al.* (2014)[4]
- **FF5** : T. Weng and J. R. Schmidt (2019)[5]

Functional forms

The starting point of development for all force fields used in this study is the General AMBER Force Field (GAFF).[6] This force field was proposed for the modelling of biomolecules, and therefore is able to describe the organic linker of ZIF-8 well. The connection of the linker with the metal is what needs custom parameterization and it represents the biggest difference between these force fields.

In FF1, the bonded and non-bonded interactions between framework atoms are modelled according to the following terms:

$$\begin{aligned} E_{\text{bonded}} = & \sum_{\text{bonds}} \frac{1}{2} K_r (r - r_0)^2 + \sum_{\text{angles}} \frac{1}{2} K_\theta (\theta - \theta_0)^2 \\ & + \sum_{\text{dihedrals}} K_\phi [1 + \cos(m\phi - \phi_0)] + \sum_{\text{impropers}} \frac{1}{2} K_\xi (\xi - \xi_0)^2 \end{aligned} \tag{1}$$

$$E_{\text{non-bonded}} = \sum 4\epsilon_{ij} \left[\left(\frac{\sigma_{ij}}{r_{ij}} \right)^{12} - \left(\frac{\sigma_{ij}}{r_{ij}} \right)^{6} \right] + \sum \frac{q_i q_j}{4\pi\epsilon_0 r} \tag{2}$$

For the bonded contribution r, θ, φ, ξ are the bond lengths and angles, proper and improper dihedrals, respectively, K_r, K_θ, K_φ, K_ξ are the force constants, and r_0, θ_0, φ_0, ξ_0 are the equilibrium values. Canonically, GAFF handles the improper torsions through the same formulation as the dihedral torsions, using a fourier-like potential. FF1, instead, opts to use a harmonic potential. The non-bonded contribution includes the Lennard-Jones and Coulombic potentials, where σ_{ij} is the collision diameter, ε_{ij} is the well depth, q_i and q_j are the atomic charges and ϵ_0 is the vacuum permittivity. The FF1 paper reports using a L-J interaction cutoff radius of 14Å, although it doesn't specify whether the potential was shifted to 0 after truncation or if tail corrections were considered. Electrostatic interactions were reported as treated with the particle mesh Ewald method, with no cutoff specified to distinguish between direct and reciprocal-space calculations. For each framework atom, a "scaled 1-4" policy was applied, that is, both the VdW and electrostatic interactions between couples of bonded atoms (1-2) or between atoms bonded to a common atom (1-3) are excluded, and for the interaction between atoms separated by two other atoms (1-4) a scaling of 0.5 and 0.8333 is applied, respectively (Figure S1).

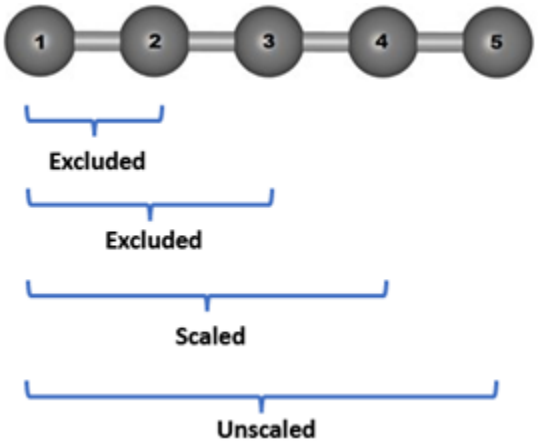

Figure S1: Pictorial representation of the 1-4 scaling policy for non-bonded interactions.

FF2, FF3 and FF4 all use the same functional form for the energy equation, the unmodified GAFF, where the improper torsions are handled using a fourier-like potential. The

bonded and non-bonded interactions between framework atoms are modelled according to the following terms:

$$E_{\text{bonded}} = \sum_{\text{bonds}} \frac{1}{2} K_r (r - r_0)^2 + \sum_{\text{angles}} \frac{1}{2} K_\theta (\theta - \theta_0)^2 + \sum_{\text{dihedrals}} K_\phi [1 + \cos(m\phi - \phi_0)] + \sum_{\text{impropers}} K_\xi [1 + \cos(m\xi - \xi_0)] \tag{3}$$

$$E_{\text{non-bonded}} = \sum 4\epsilon_{ij} \left[\left(\frac{\sigma_{ij}}{r_{ij}} \right)^{12} - \left(\frac{\sigma_{ij}}{r_{ij}} \right)^{6} \right] + \sum \frac{q_i q_j}{4\pi\epsilon_0 r} \tag{4}$$

The FF2 paper reports using a L-J interaction cutoff radius of 14Å, although it doesn't specify whether the potential was shifted to 0 after truncation or if tail corrections were considered. Electrostatic interactions were reported as treated with the particle mesh Ewald method with a grid spacing of 1.2 Å and a fourth-order interpolation, however no cutoff was specified to distinguish between direct and reciprocal-space calculations. The use of a 1-4 non-bonded interaction policy for closely bonded atoms is not mentioned.

The FF3 paper, written by the same authors as FF2, does not provide information regarding non-bonded interaction cutoffs, long-range treatment or 1-4 non-bonded interaction policy.

The FF4 paper reports using a L-J interaction cutoff radius of 14Å, although it doesn't specify whether the potential was shifted to 0 after truncation or if tail corrections were considered. Electrostatic interactions were reported as treated via the particle mesh Ewald method, with no cutoff specified to distinguish between direct and reciprocal-space calculations. A scaled 1-4 interaction policy was used in which 1-2 and 1-3 interactions are excluded and scaling values of 0.5 for both the 1-4 coulombic and VdW interactions are considered.

FF5 makes use of the same functional forms, but includes an Urey-Bradley term as part of the 3-body angular potential. The bonded and non-bonded interactions between framework atoms are modelled according to the following terms:

$$E_{\text{bonded}} = \sum_{\text{bonds}} \frac{1}{2} K_r (r - r_0)^2 + \sum_{\text{angles}} \frac{1}{2} K_\theta (\theta - \theta_0)^2 + \sum_{\text{Urey-Bradley}} \frac{1}{2} K_u (u - u_0)^2 + \sum_{\text{dihedrals}} K_\phi [1 + \cos(m\phi - \phi_0)] + \sum_{\text{impropers}} K_\xi [1 + \cos(m\xi - \xi_0)] \quad (5)$$

$$E_{\text{non-bonded}} = \sum 4\epsilon_{ij} \left[\left(\frac{\sigma_{ij}}{r_{ij}} \right)^{12} - \left(\frac{\sigma_{ij}}{r_{ij}} \right)^{6} \right] + \sum \frac{q_i q_j}{4\pi\epsilon_0 r} \quad (6)$$

The paper reports using a L-J interaction cutoff radius of 13Å with long-range tail corrections considered. Electrostatic interactions were reported as treated via the particle-particle particle-mesh (PPPM) method, with a cutoff radius of 13Å. A 1-4 scaling 0.6874 factor for coulombic interactions was reported. The 1-4 scaling factor for VdW interactions was not explicitly reported in the paper, however, in the files provided as part of the supporting information the conventional choice for GAFF (0.5) is used. As was the case for other force fields, as part of the 1-4 scaling policy, 1-2 and 1-3 non-bonded interactions are excluded.

Parameter sets

The tables included in this subsection contain the interaction parameters used in this work for the previously described force fields. The atom types referenced in the text and tables are labeled in a standardized manner according to the pictured nomenclature (Figure S2).

The parameters for FF1 contained in the tables were taken directly from the original paper, including the changes published by the authors in a subsequent erratum concerning the VdW σ parameter for H3 and the partial charge for C3. According to the paper, the parameters for the organic linker not included in the "parm10.dat" AMBER database were obtained via the parmcal program of the Antechamber package.[7] The bond-length and bond-angle parameters involved in interactions of tetrahedral ZnN_4 were taken and adapted from a couple of quantum-chemical studies describing Zn-containing biomolecules for AMBER.[8,9] The VdW parameters for Zn were taken from the work of Mertz *et al.*,[10] which some of the AMBER parameter databases include. The partial charges were obtained via density

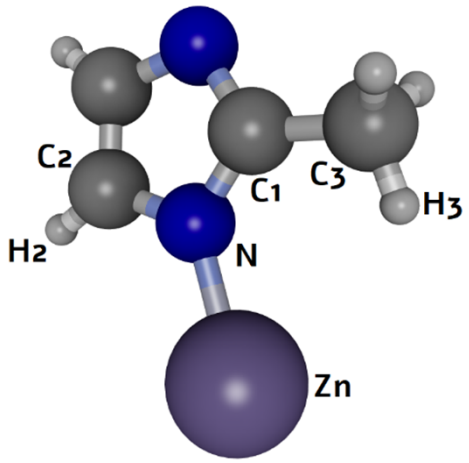

Figure S2: Atom nomenclature used in this work.

functional theory calculations on finite clusters previously published by the same research group.[11] In the parametrization presented by the paper the torsion terms N-Zn-N-C1, N-Zn-N-C2 and N-C1-C3-H3 were neglected, to ensure higher mobility of the organic linkers with respect to each other and to allow free rotation of the methyl group in the linker, respectively. As far as we can tell, the Zn-containing torsion terms Zn-N-C2-H2, Zn-N-C2-C2, C3-C1-N-Zn and N-C1-N-Zn were considered and modelled the same way as the purely organic torsions, via the X-CR-NB-X, X-CC-CV-X and X-CR-NA-X (where X denotes generic entries, any atom) interaction parameters located in the "parm10.dat" database. The parameters for the improper torsions used are missing in the database, therefore it can be assumed they were calculated using the parmcal program.

The parameters for FF2 contained in the tables were taken directly from the original paper, including the changes published by the authors in a subsequent erratum concerning the correct equilibrium bond lengths r_0 of C2-H2 and C3-H1. According to the paper, the equilibrium bond lengths and angles for all bonded interactions were set to the experimentally measured average values. The force constants for the organic linkers were adopted from the AMBER force field (no specific database mentioned), while those involving Zn atoms were derived by fitting to experimental lattice constants. The non-bonded Lennard-Jones parameters for all atoms were taken from the AMBER force field (no specific database file

Table S1: Non-bonded interaction parameters.

		FF1	**FF2**	**FF3**	**FF4**	**FF5**
	ϵ	0.17	0.17	0.0373	0.0438	0.17
N	σ	3.25	3.25	3.261	3.261	3.25
	q	-0.3008	-0.5	-0.28	-0.3879	-0.4203
	ϵ	0.086	0.086	0.0567	0.0667	0.086
C1	σ	3.4	3.4	3.431	3.431	3.4
	q	0.4339	0.5	0.4184	0.4291	0.4375
	ϵ	0.086	0.086	0.0567	0.0667	0.086
C2	σ	3.4	3.4	3.431	3.431	3.4
	q	-0.1924	-0.1	-0.191	-0.0839	-0.0662
	ϵ	0.1094	0.1094	0.0567	0.0667	0.086
C3	σ	3.4	3.4	3.431	3.431	3.4
	q	-0.6042	-0.3	-0.5726	-0.4526	-0.4606
	ϵ	0.015	0.015	0.0238	0.0279	0.015
H2	σ	2.511	2.421	2.571	2.571	2.51
	q	0.1585	0.1	0.1536	0.1128	0.1141
	ϵ	0.0157	0.0157	0.0238	0.0279	0.0157
H3	σ	2.471	2.65	2.571	2.571	2.471
	q	0.1572	0.1	0.1481	0.1325, 0.1306	0.1381
	ϵ	0.0125	0.0125	0.067	0.0787	0.0125
Zn	σ	1.96	1.96	2.462	2.462	1.96
	q	0.7362	1.0	0.6894	0.6918	0.7072

ϵ in $kcal/mol$; σ in Å; q in e

mentioned). The atomic charges were obtained via DFT calculations using a fragmental cluster model, previously published by the same research group.[12] It is worth noting that the charge values presented in the FF2 paper and those from the referenced paper differ slightly, and no reason was given to justify said change. In this work we used the ones published with the proposed FF.[2]

It's worth mentioning that although the LJ parameters for both FF1 and FF2 were taken from AMBER databases, their values are not the same for all atoms, as can be seen in Table S1. This is due to the atom model selection each paper employs. For example, FF1 models H2 as an aromatic hydrogen bonded to a carbon atom with 1 electron-withdrawing group (denoted as H4 in AMBER databases) while FF2 models H2 as an aromatic hydrogen bonded to a carbon atom with 2 electron-withdrawing groups (denoted as H5 in AMBER

Table S2: Bond stretching interaction parameters.

		FF1	**FF2**	**FF3**	**FF4**	**FF5**
C1-C3	K_r	693.086	634	634	634	451.26
	r_0	1.49	1.493	1.492	1.492	1.498
C1-N	K_r	976	976	976	976	674.52
	r_0	1.335	1.34	1.339	1.339	1.355
C2-N	K_r	880.42	820	820	820	579.3
	r_0	1.37	1.371	1.371	1.3711	1.386
C2-H2	K_r	734	734	734	734	739.5
	r_0	1.08	0.929	0.929	0.929	1.088
C2-C2	K_r	1080.50	1036	1036	1036	804.64
	r_0	1.35	1.346	1.346	1.346	1.377
C3-H3	K_r	680	680	680	680	643.54
	r_0	1.09	0.96	0.959	0.959	1.102
Zn-N	K_r	157	167.304	172	172	149
	r_0	2.011	1.987	1.987	1.987	2.024

K_r in $kcal \cdot mol^{-1} \cdot \text{Å}^{-2}$; r_0 in Å;

databases), hence there's a difference in the σ LJ parameter. The previous observation applies for all discussed force fields, meaning that if the parameters from different FFs were said to be taken from the GAFF force field, and, when comparing between them, they are not exactly the same; it's usually due to decisions relating to the atom model selection.

The parameters for FF3 contained in the tables were taken directly from the original paper. According to it, the equilibrium bond lengths and angles for all bonded interactions were set to the experimentally measured average values. The force constants of the bonded interactions for the organic linkers were adopted from the AMBER force field (no specific database file mentioned). Regarding the ZnN_4 tetrahedra, the force constant for the N-Zn bond was adopted from a parameter-optimization study intended for the Molecular Mechanics (MM2) force field[13] and the force constants for C1-N-Zn and C2-N-Zn were taken from the work of Lin and Wang.[9] For N-Zn-N bending and the torsional terms Zn-N-C1-N, Zn-N-C1-C3 and Zn-N-C2-C2 the force constants were adopted from FF2. Unlike the previous two force fields, FF3 was specifically tuned to study the structural transition of ZIF-8 upon N_2 loading. The N-Zn-N-C1 and N-Zn-N-C2 force constants were fitted to experimental data of

Table S3: Angle bending interaction parameters.

		FF1	**FF2**	**FF3**	**FF4**	**FF5**
N-C1-N	K_θ	150.968	140	140	140	64.68
	θ_0	112.16	112.17	112.17	112.17	111.169
N-C1-C3	K_θ	132.03	140	140	140	78.14
	θ_0	123.92	123.89	1123.89	123.89	124.197
C2-C2-N	K_θ	147.5	140	140	140	67.16
	θ_0	108.65	108.67	108.67	108.67	107.995
C2-C2-H2	K_θ	98.902	100	100	100	38.78
	θ_0	125.67	125.67	125.67	125.67	130.034
N-C2-H2	K_θ	99.908	100	100	100	63.16
	θ_0	125.68	125.66	125.66	125.66	121.317
C1-N-C2	K_θ	142.508	140	140	140	92.66
	θ_0	105.27	105.24	105.24	105.24	106.252
C1-C3-H3	K_θ	96.176	100	100	100	72.62
	θ_0	109.32	109.44	109.44	109.44	110.963
H3-C3-H3	K_θ	70	70	70	70	54.36
	θ_0	109.5	109.5	109.5	109.5	107.741
C1-N-Zn	K_θ	97.36	40.631	100	100	28.86
	θ_0	128.33	128.35	127.5	127.5	126.85
C2-N-Zn	K_θ	64.954	43.021	70	70	22.72
	θ_0	126.4	126.4	128	128	126.95
N-Zn-N	K_θ	70.48	23.9	21	21	22.18
	θ_0	109.48	109.47	109.47	109.47	109.42

K_θ in $kcal \cdot mol^{-1} \cdot rad^{-2}$; θ_0 in deg;

the N_2 sorption isotherm.[14] The LJ parameters were adopted from the universal force field[15] with the well depth parameters ϵ rescaled by a factor of 0.54, in order to better reproduce the adsorption isotherm of N_2. The atomic charges were adopted from previously published plane-wave DFT calculations on a periodic structure.[11]

The parameters for FF4 contained in the tables were taken directly from the original paper. According to it, the equilibrium bond lengths and angles for all bonded interactions were set to the experimentally measured average values. The force constants of the bonded interactions for the organic linkers were adopted from the AMBER force field (no specific database file mentioned). All bonded interaction parameters involving Zn were taken from FF3. This force field was tuned to study diffusion and adsorption of N_2, CH_2, CO_2 and

Table S4: Urey-Bradley interaction parameters.

		FF5
N-C1-N	K_u	214.74
	u_0	2.236
N-C1-C3	K_u	61.22
	u_0	2.522
C2-C2-N	K_u	198.1
	u_0	2.235
C2-C2-H2	K_u	29.56
	u_0	2.236
N-C2-H2	K_u	40.86
	u_0	2.16
C1-N-C2	K_u	223.3
	u_0	2.193
C1-C3-H3	K_u	38.32
	u_0	2.153
H3-C3-H3	K_u	37.34
	u_0	1.779
C1-N-Zn	K_u	0
	u_0	0
C2-N-Zn	K_u	0
	u_0	0
N-Zn-N	K_u	0
	u_0	0

K_u in $kcal \cdot mol^{-1} \cdot$ Å^{-2}; u_0 in Å;

CH_4 and as was the case with the previous force field, the LJ parameters were adopted from the universal force field[15] but with the well depth ϵ rescaled by a factor of 0.635. The partial charges were computed by using the density-derived electrostatic and chemical charge method (DDEC). The paper provides 2 values for the charge of H3 atoms and does not specify which value or combination of values was used for their simulations. We found that in order to obtain a charge-neutral framework, two of the H3 hydrogens in the methyl group must have a charge of 0.1306e (first value in Table S1) and the other H3 hydrogen must have a charge of 0.1306 (second value in Table S1).

The parameters for FF5 contained in the tables were taken directly from the original paper. The parameters of the bonded interactions for the organic linkers were adopted

Table S5: Improper torsion interaction parameters.

		FF2	FF3	FF4	FF5
N-C1-N-C3	K_ξ [a]	1.1	1.1	1.1	3.5
	m	2	2	2	2
	ξ_0	180	180	180	180
N-C2-C2-H2	K_ξ [a]	1.1	1.1	1.1	0
	m	2	2	2	2
	ξ_0	180	180	180	180
Zn-N-C1-C2	K_ξ [a]	0.0956	—	—	0.056
	m	2	—	—	2
	ξ_0	180	—	—	180

		FF1
N-C1-N-C3	K_ξ [b]	4
	ξ_0	180
N-C2-C2-H2	K_ξ [b]	4
	ξ_0	180
Zn-N-C1-C2	K_ξ [b]	4
	ξ_0	180

[a] in $kcal/mol$; [b] in $kcal \cdot mol^{-1} \cdot rad^{-2}$; ξ_0 in deg; 2nd atom is the central one

from the work of Gabrieli *et al.*[16] who optimized the GAFF originals on the basis of force matching. All bonded interaction parameters involving Zn were re-optimized by the authors against DFT-calculated properties using a genetic algorithm. The LJ parameters were taken directly from GAFF while the partial charges were computed using DDEC.

Additional details

The force fields were implemented as close as stated by the original papers as possible, however, as mentioned in section 1.2 some of them do not include crucial information. For example, if not stated explicitly by the article, the cutoff for direct electrostatic calculations in our simulations was set to 12.0 Å. A summary of the cutoffs and 1-4 scaling parameters used in this work is provided in Table S8. In order to determine the 1-4 non-bonded interaction scaling parameters for FF2, a series of NPT MD simulations were run using a variety of classical FF scaling policies, specifically, those of AMBER (0.5 for VdW, 0.8333 for electrostatic), Dreiding (both unscaled) CHARMM (0 for both) and OPLS/AA (0.5 for both). The average lattice parameters of the unit cell were subsequently computed and compared to those reported by the authors. We found that a 1-4 scaling policy of 0.5 for both VdW and electrostatic interactions provided the reported average lattice parameter value of $\approx$ 17.0 Å.

For FF3, a VdW interaction cutoff of 14.0 Å and 1-4 scaling policy of 0.5 for both VdW

Table S6: Dihedral torsion interaction parameters.

		FF1	**FF2**	**FF3**	**FF4**	**FF5**
C1-N-C2-H2	K_ϕ	2.325	4.8	4.8	4.8	3.65
	m	2	2	2	2	2
	ϕ_0	180	180	180	180	180
C1-N-C2-C2	K_ϕ	2.325	4.8	4.8	4.8	6.64
	m	2	2	2	2	2
	ϕ_0	180	180	180	180	180
N-C2-C2-H2	K_ϕ	5.15	4	4	4	3.55
	m	2	2	2	2	2
	ϕ_0	180	180	180	180	180
N-C2-C2-N	K_ϕ	5.15	4	4	4	15.33
	m	2	2	2	2	2
	ϕ_0	180	180	180	180	180
H2-C2-C2-H2	K_ϕ	5.15	4	4	4	0.34
	m	2	2	2	2	2
	ϕ_0	180	180	180	180	180
C3-C1-N-C2	K_ϕ	5	4.8	4.15	4.15	3.64
	m	2	2	2	2	2
	ϕ_0	180	180	180	180	180
N-C1-N-C2	K_ϕ	5	4.8	4.8	4.8	10.77
	m	2	2	2	2	2
	ϕ_0	180	180	180	180	180
N-C1-C3-H3	K_ϕ	—	—	—	—	0.27
	m	—	—	—	—	2
	ϕ_0	—	—	—	—	180

K_ϕ in $kcal/mol$; ϕ_0 in deg

and electrostatic interactions were tested and found to reproduce the geometric properties of the unit cell reported by the paper. Said values were selected for analysis based on the fact that FF3 was created by the same group that proposed FF2. As previously stated, FF5 does not explicitly report on the 1-4 scaling parameter for VdW interactions, however, the simulation files provided as supporting documentation use a value of 0.5 and therefore we do too.

Table S7: Dihedral torsions involving Zn.

		FF1	**FF2**	**FF3**	**FF4**	**FF5**
Zn-N-C2-H2	K_ϕ	2.325	0.12	—	—	1.056
	m	2	2	—	—	2
	ϕ_0	180	180	—	—	180
Zn-N-C2-C2	K_ϕ	2.325	0.12	0.1	0.1	1.416
	m	2	2	2	2	2
	ϕ_0	180	180	180	180	180
C3-C1-N-Zn	K_ϕ	5	0.12	0.1	0.1	0.227
	m	2	2	2	2	2
	ϕ_0	180	180	180	180	180
N-C1-N-Zn	K_ϕ	5	0.12	0.1	0.1	0.614
	m	2	2	2	2	2
	ϕ_0	180	180	180	180	180
N-Zn-N-C1	K_ϕ	—	—	0.174	0.174	0.026
	m	—	—	3	3	3
	ϕ_0	—	—	0	0	0
N-Zn-N-C2	K_ϕ	—	—	0.174	0.174	0.021
	m	—	—	3	3	3
	ϕ_0	—	—	0	0	180

K_ϕ in $kcal/mol$; ϕ_0 in deg

Table S8: Interaction cutoff values and 1-4 scaling parameters

	VdW r_{cut}	Elec. r_{cut}	VdW 1-4 scaling	Elec. 1-4 scaling
FF1	14.0	12.0	0.50	0.8333
FF2	14.0	12.0	0.50	0.50
FF3	14.0	12.0	0.50	0.50
FF4	14.0	12.0	0.50	0.50
FF5	13.0	13.0	0.50	0.6875

r_{cut} in Å

Force field implementation

Potential functions

The potential terms defined in the original papers are available in both the RASPA and LAMMPS simulation packages, thus one can produce a faithful adaptation without the need to resort to any approximate functions. Care must be taken when writing-in the FF parameters, as the default input energy units for each code is different.

The bond stretching term is provided as the "harmonic" bond_style in LAMMPS and the "HARMONIC_BOND" potential in RASPA. The usual 1/2 factor is included in the force constant in the former while it's not in the latter.

The harmonic angle bending term is provided as the "harmonic" angle_style in LAMMPS and the "HARMONIC_BEND" potential in RASPA. As is the case with the previous potential type, the usual 1/2 factor is included in the force constant in LAMMPS while it is not in RASPA. For FF5, where the bending potential includes both a harmonic and Urey-Bradley contribution, LAMMPS provides the "charmm" angle_style which encompasses both. RASPA requires the separate inclusion of the U-B term "HARMONIC_UREYBRADLEY" in addition to the canonical harmonic bend.

The Fourier-style dihedral torsion is provided as the "charmm" dihedral_style in LAMMPS (with a 'weighing factor' of 0.0) and the "CVFF_DIHEDRAL" potential in RASPA. The harmonic improper torsion is provided as the "harmonic" improper_style in LAMMPS and the "HARMONIC_IMPROPER_DIHEDRAL" potential in RASPA. The usual 1/2 factor is included in the force constant in LAMMPS while it is not in RASPA. The Fourier-style improper torsion is provided as "cvff" in LAMMPS and as "CVFF_IMPROPER_DIHEDRAL" in RASPA.

Simulation code congruency verification

In order to employ the two-code approach for the analysis and comparison of structural and mechanical properties, it is necessary to first verify that the FF implementations provide congruent results between the codes. For this, the term-by term contributions to the energy were calculated with both codes, for the same atomic configuration.

A system consisting of 8 (2X2X2) unit cells of ZIF-8 was employed in the RASPA simulations, using the unit cell crystallographic information file (CIF) constructed by D. Dubbeldam based on previously reported experimental measurements by K. S. Park, *et al.*[17] The input topologies for LAMMPS were created using an in-house script using the atomic po-

sitions from the same CIF and the framework atom connectivity information inferred from each force field. The reason for using CIF instead of the more ubiquitous PDB file is that the latter only allows for the representation of max. 3 decimal numbers.

Table S9: Initial configuration energy contributions comparison of RASPA vs LAMMPS.

		Bond	**Bend**	**Torsion**	**Improper**	**VdW**	**Coulomb**
FF1[1]	L	6546.2087	0.58568845	17.604775	1.2026054	-1297.5469	-6623.2763
	R	6546.208735	0.585688452	17.60477513	1.202605444	-1297.54688	-6623.114704
FF2[2]	L	0.38769074	0.17431773	12.203572	0.79748426	-1269.003	1793.179
	R	0.387690631	0.174320676	12.21174146	0.797485075	-1269.02699	1793.198783
FF3[3]	L	0.32090403	14.967566	417.93868	0.76345557	-840.44983	3181.5197
	R	0.320904031	14.96756588	417.9386731	0.763455565	-840.4498429	3181.594673
FF4[4]	L	0.32090403	14.967566	417.93868	0.95044739	-987.47822	1379.6331
	R	0.320904031	14.96756588	417.9386777	0.950447386	-987.4782257	1379.68962
FF5[5]	L	7500.0047	1243.3146	326.53627	2.4490301	-1243.3647	-6434.1725
	R	7500.004681	1243.314574	326.5362699	2.449030136	-1243.364629	-6434.159446

Units of kcal $\cdot$ mol^{-1}; L is LAMMPS, R is RASPA

As can be seen in Table S9 the energy terms of each contribution match up to at least the fourth decimal in the case of bonded and VdW interactions and up to the second decimal in the case of electrostatic interactions. The differences in the latter might be due to either different implementations of the Ewald summation in the codes or the finite precision of the specified atom positions.

Additional results

Temperature dependence

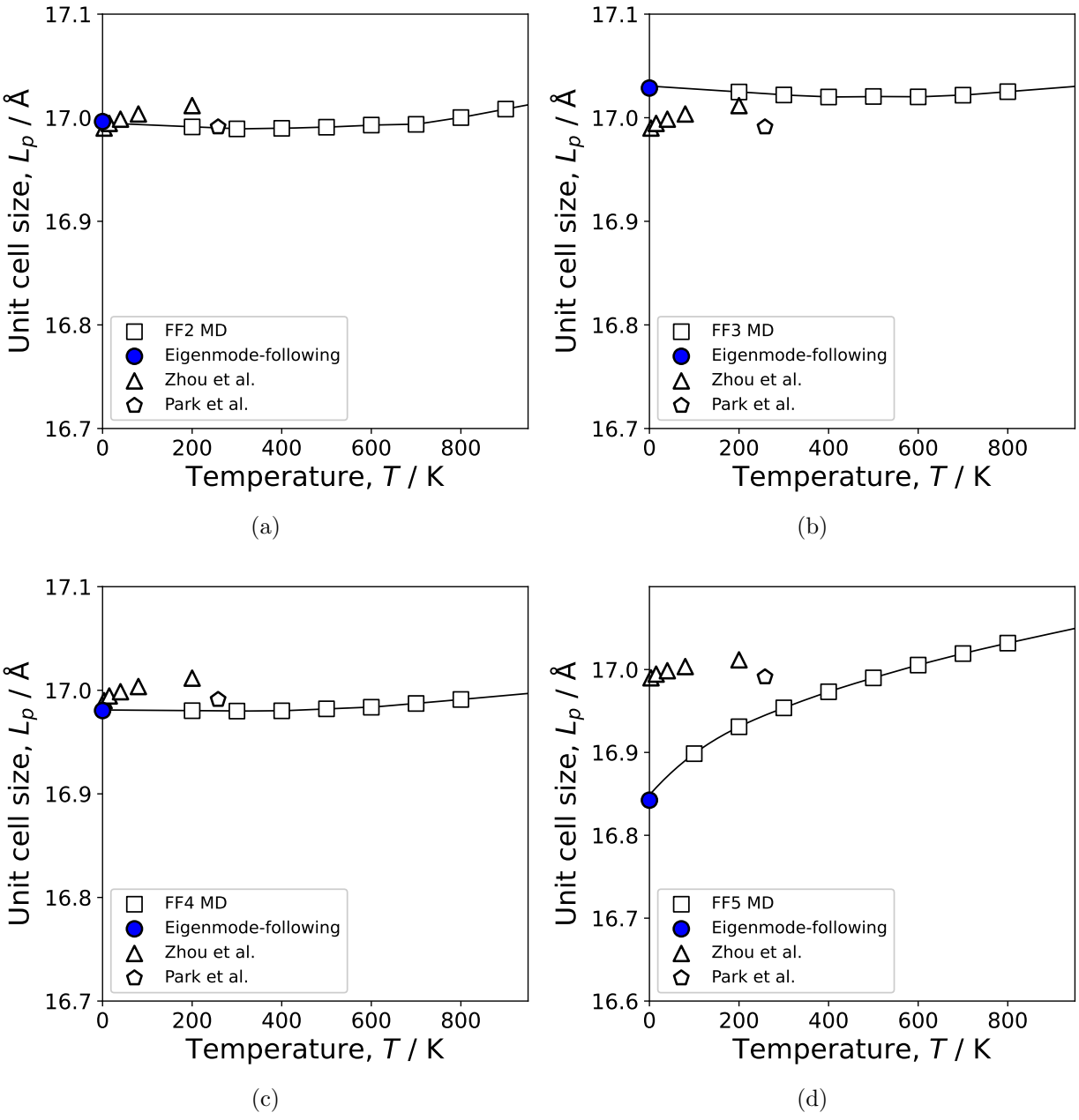

Figure S3: Size of the unit cell of ZIF-8 predicted by FF2-FF4. MD data obtained at a pressure of 1atm and represented with open squares. Experimental measurements from Park et al.[17] (XRD) and Zhou et al.[18] (neutron HRPD) represented with stars and triangles, respectively. Extrapolated values at 0K are compared with the unit cell size obtained using Eigenmode-following minimization technique.

Pressure dependence of the unit cell

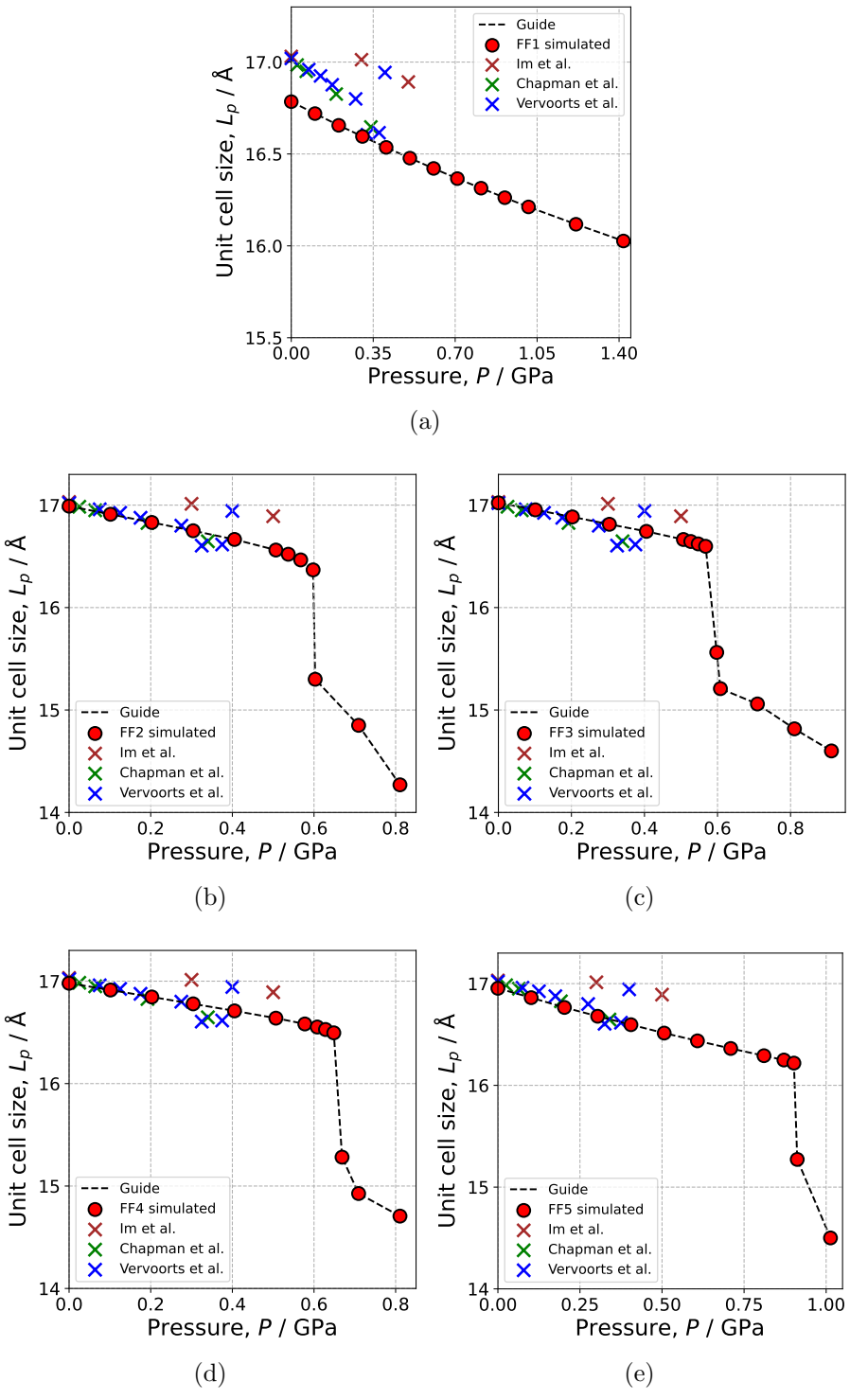

Figure S4: Pressure dependence isotherms (T=300K) of the unit cell lattice parameter for the implemented force fields. Reported experimental measurements represented as crosses.[19–21]

References

(1) Zheng, B.; Sant, M.; Demontis, P.; Suffritti, G. B. Force Field for Molecular Dynamics Computations in Flexible ZIF-8 Framework. *The Journal of Physical Chemistry C* **2012**, *116*, 933–938.

(2) Hu, Z.; Zhang, L.; Jiang, J. Development of a force field for zeolitic imidazolate framework-8 with structural flexibility. *The Journal of Chemical Physics* **2012**, *136*, 244703.

(3) Zhang, L.; Hu, Z.; Jiang, J. Sorption-Induced Structural Transition of Zeolitic Imidazolate Framework-8: A Hybrid Molecular Simulation Study. *Journal of the American Chemical Society* **2013**, *135*, 3722–3728.

(4) Wu, X.; Huang, J.; Cai, W.; Jaroniec, M. Force field for ZIF-8 flexible frameworks: atomistic simulation of adsorption, diffusion of pure gases as CH4, H2, CO2 and N2. *RSC Adv.* **2014**, *4*, 16503–16511.

(5) Weng, T.; Schmidt, J. R. Flexible and Transferable ab Initio Force Field for Zeolitic Imidazolate Frameworks: ZIF-FF. *The Journal of Physical Chemistry A* **2019**, *123*, 3000–3012.

(6) Wang, J.; Wolf, R. M.; Caldwell, J. W.; Kollman, P. A.; Case, D. A. Development and testing of a general amber force field. *Journal of Computational Chemistry* **2004**, *25*, 1157–1174.

(7) Wang, J.; Wang, W.; Kollman, P. A.; Case, D. A. Automatic atom type and bond type perception in molecular mechanical calculations. *Journal of Molecular Graphics and Modelling* **2006**, *25*, 247–260.

(8) Peters, M. B.; Yang, Y.; Wang, B.; Füsti-Molnár, L.; Weaver, M. N.; Merz, K. M.

Structural Survey of Zinc-Containing Proteins and Development of the Zinc AMBER Force Field (ZAFF). *Journal of Chemical Theory and Computation* **2010**, *6*, 2935–2947.

(9) Lin, F.; Wang, R. Systematic Derivation of AMBER Force Field Parameters Applicable to Zinc-Containing Systems. *Journal of Chemical Theory and Computation* **2010**, *6*, 1852–1870.

(10) Hoops, S. C.; Anderson, K. W.; Merz, K. M. Force field design for metalloproteins. *Journal of the American Chemical Society* **1991**, *113*, 8262–8270.

(11) Rana, M. K.; Pazzona, F. G.; Suffritti, G. B.; Demontis, P.; Masia, M. Estimation of Partial Charges in Small Zeolite Imidazolate Frameworks from Density Functional Theory Calculations. *Journal of Chemical Theory and Computation* **2011**, *7*, 1575–1582.

(12) Hu, Z.; Chen, Y.; Jiang, J. Zeolitic imidazolate framework-8 as a reverse osmosis membrane for water desalination: Insight from molecular simulation. *The Journal of Chemical Physics* **2011**, *134*, 134705.

(13) Marques, H. M.; Cukrowski, I. Molecular mechanics parameters for the modelling of four-coordinate Zn(ii) porphyrins. *Phys. Chem. Chem. Phys.* **2003**, *5*, 5499–5506.

(14) Fairen-Jimenez, D.; Moggach, S. A.; Wharmby, M. T.; Wright, P. A.; Parsons, S.; Düren, T. Opening the Gate: Framework Flexibility in ZIF-8 Explored by Experiments and Simulations. *Journal of the American Chemical Society* **2011**, *133*, 8900–8902.

(15) Rappe, A. K.; Casewit, C. J.; Colwell, K. S.; Goddard, W. A.; Skiff, W. M. UFF, a full periodic table force field for molecular mechanics and molecular dynamics simulations. *Journal of the American Chemical Society* **1992**, *114*, 10024–10035.

(16) Gabrieli, A.; Sant, M.; Demontis, P.; Suffritti, G. B. Fast and efficient optimization

of Molecular Dynamics force fields for microporous materials: Bonded interactions via force matching. *Microporous and Mesoporous Materials* **2014**, *197*, 339–347.

(17) Park, K. S.; Ni, Z.; Côté, A. P.; Choi, J. Y.; Huang, R.; Uribe-Romo, F. J.; Chae, H. K.; O'Keeffe, M.; Yaghi, O. M. Exceptional chemical and thermal stability of zeolitic imidazolate frameworks. *Proceedings of the National Academy of Sciences* **2006**, *103*, 10186–10191.

(18) Zhou, W.; Wu, H.; Udovic, T. J.; Rush, J. J.; Yildirim, T. Quasi-Free Methyl Rotation in Zeolitic Imidazolate Framework-8. *The Journal of Physical Chemistry A* **2008**, *112*, 12602–12606.

(19) Chapman, K. W.; Halder, G. J.; Chupas, P. J. Pressure-Induced Amorphization and Porosity Modification in a Metal-Organic Framework. *Journal of the American Chemical Society* **2009**, *131*, 17546–17547.

(20) Vervoorts, P.; Burger, S.; Hemmer, K.; Kieslich, G. Revisiting the High-Pressure Properties of the Metal-Organic Frameworks ZIF-8 and ZIF-67. **2020**,

(21) Im, J.; Yim, N.; Kim, J.; Vogt, T.; Lee, Y. High-Pressure Chemistry of a Zeolitic Imidazolate Framework Compound in the Presence of Different Fluids. *Journal of the American Chemical Society* **2016**, *138*, 11477–11480.